ADVANCED MODELING AND COMPUTATIONAL METHODS FOR DISTRIBUTION SYSTEM STATE ESTIMATION

BY

CECILIA KLAUBER

THESIS

Submitted in partial fulfillment of the requirements
for the degree of Master of Science in Electrical and Computer Engineering
in the Graduate College of the
University of Illinois at Urbana-Champaign, 2016

Urbana, Illinois

Adviser:

Assistant Professor Hao Zhu

ABSTRACT

Growing penetration of distributed energy resources and smart grid technologies interfacing with the power distribution network motivate the continued advancement of accurate and robust system monitoring tools. Traditional state estimation approaches rely on iterative methods to solve the weighted least squares problem because of the nonlinear relationship between the power measurements and voltage phasor state. It is known that these methods may be prone to convergence and numeric instability issues, such as in the presence of a measurement set of diverse quality. In this thesis, distribution system state estimation techniques are developed to address this monitoring need and take advantage of recent interest in alternative power flow models for distribution systems and convex and quadratic optimization methods. Therefore, semidefinite and quadratic programming methods, enabled by alternative power flow models, are leveraged to provide accurate solutions that are robust to various measurement types yet computationally efficient.

The first proposed method employs a reformulation of the power flow measurement equations that captures the quadratic relationship between power and voltage. The state estimation problem is cast as a semidefinite program and gains the desirable convergence and solution accuracy characteristics therein. This method attains near-optimal performance without suffering from the numerical issues caused by variety of measurement quality, specifically the inclusion of virtual measurements at zero-injection nodes. The second method utilizes linearized power flow equations to cast the problem as a quadratic program with linear constraints. With minimal added computational complexity, the estimate is improved by including approximations of the nonlinear terms ignored during the linearized model development. This method also efficiently provides a reliable state estimate while avoiding the ill-conditioning issues that plague the traditional iterative methods. Numer-

ical tests have been successfully performed on the IEEE 13-bus and 123-bus case studies.

To my family, for their love and support.

ACKNOWLEDGMENTS

I would like to thank my advisor, Hao Zhu, for her support and guidance. I am continually inspired by her tenacity, passion, and dedication to research excellence, and I am truly grateful for the opportunity to continue my education under her guidance. I am grateful to the professors, students, and staff of the University of Illinois Power and Energy Systems Group. It has been a joy and an honor to work alongside you all.

I would like to acknowledge the College of Engineering, the Carver Foundation, and the National Science Foundation Graduate Research Fellowship for financial support of this work.

Finally, I would like to thank my friends and family for all the encouragement and support over the years.

TABLE OF CONTENTS

LIST OF TABLES vii

LIST OF FIGURES viii

CHAPTER 1 INTRODUCTION 1
1.1 Motivation and Context 1
1.2 Thesis Contributions and Outline 5

CHAPTER 2 SEMIDEFINITE PROGRAMMING FOR DSSE 7
2.1 Matrix Representation for Multi-Phase Power Flow 7
2.2 SDP-based State Estimation 8
2.3 Chapter Summary 11

CHAPTER 3 LINEAR POWER FLOW MODELING FOR DSSE . . 12
3.1 Modeling of Single- and Multi-Phase Networks 12
3.2 Comparison of the Linear Models 17
3.3 LDF-based State Estimation 20
3.4 Chapter Summary 24

CHAPTER 4 SIMULATION RESULTS 25
4.1 SDP-based State Estimation Results 25
4.2 LDF-based State Estimation Results 29
4.3 Chapter Summary 35

CHAPTER 5 CONCLUSION 37
5.1 Future Work 38

REFERENCES 39

LIST OF TABLES

4.1 Euclidean norm estimation error results of the SDP SE scheme for the 13-bus system 26
4.2 Euclidean norm estimation error results of the SDP SE scheme for the 13-bus system with bad data 28
4.3 The rMSE results of the four LDF-based SE schemes for the 13-bus system 30
4.4 The rMSE results of LDF-based SE schemes for the 123-bus system 34
4.5 Actual and estimated transformer tap ratio and position for one instance of the 123-bus results 35

LIST OF FIGURES

3.1 An example of a radial feeder 13
3.2 Voltage magnitude error of single-phase model for the simplified 123-bus feeder 18
3.3 Voltage magnitude error of multi-phase model for the IEEE 13-bus feeder 19
3.4 Flow chart depicting the steps of the Δ-LDF:AC method . . . 21
3.5 Classical transformer model and its equivalent transformer model 24

4.1 The IEEE 13-bus test feeder 26
4.2 SDP estimation error comparison of node voltage magnitude for the 13-bus system 27
4.3 SDP estimation error comparison of node voltage angle for the 13-bus system 27
4.4 Measurement residual at every meter in the 13-bus system for SDP bad data detection 28
4.5 Absolute voltage error results of three LDF SE schemes for the 13-bus system 31
4.6 Average estimation error in (left) voltage magnitude and (right) line power flows versus the noise level in power injection measurements 32
4.7 Average estimation error in voltage magnitude versus number of measurements (out of 20) chosen to be at a higher noise variance 33
4.8 Voltage magnitude error results for the 123-bus system, by phase and distance 34
4.9 Percent of occurrences in erroneous tap estimation versus severity of error, with and without μPMU 36

CHAPTER 1

INTRODUCTION

Distribution system state estimation (DSSE) can provide a nearly real-time view of network flow and component status by processing network-wide measurement data. This situational awareness enables critical support and functionality such as system security, monitoring, and control [1]. With a rapidly growing number of distributed renewable generation sources and smart grid technologies interfacing with distribution networks, effectively obtaining the system status in a timely manner through the development of efficient and reliable state estimation (SE) methods is of increasing interest. Meanwhile, these new devices and technologies also introduce additional challenges to the DSSE problem. These obstacles include increased stress on the grid, potential for fraud or cyber attack, and complication of operations. For example, the installation of distributed energy resources, usage of electric vehicles as energy storage, and implementation of demand response programs contribute to the advent of less predictable flow patterns on the network. Where power flow was once unidirectional and predictable, comprehensive monitoring techniques are increasingly essential for effective system operations and control. In addition to the changes in physical loads and resources, the cyber infrastructure landscape has significantly advanced with improved sensing, communication, and control capabilities available to distribution system operators. Hence, there is a timely opportunity to develop advanced SE methods that can improve visibility while enhancing efficiency and reliability for distribution systems.

1.1 Motivation and Context

For bulk transmission systems, the SE problem has been extensively investigated with several established algorithms and successful implementations

[2, 3]. The SE problem becomes more challenging, however, for distribution systems due to differences in network characteristics and availability of measurements [4]. Specifically, several features of distribution systems are known to contribute to the ill-conditioning issues of Jacobian matrices for conventional power flow methods and applications. These include:

- Radial or weakly meshed topology
- High R/X ratio of line segments
- Unbalanced loads and phasing

Among these three, the unbalanced feature also challenges the computational efficiency of DSSE. Power transmission systems are often designed to be well-balanced, which allows for the symmetrical component transformation of transmission lines. Thus a single-phase representation of the network is sufficient to capture the three-phase power flow equations. In contrast, distribution systems are inherently unbalanced. This is because line conductors may not be fully transposed, loads are not always balanced, and the line segments can even be single-phase or double-phase. Accordingly, the symmetrical component transformation no longer holds and a multi-phase representation is needed for distribution system analysis. Consequently, the dimension of the problem increases, motiving the consideration of efficient computational methods to accelerate DSSE solvers.

Similar to transmission SE, DSSE can be formulated using the weighted least-squares (WLS) error criterion [5]. The WLS criterion is statistically optimal given that the measurement error is independent and Gaussian with known variance. Under the nonlinear ac power flow equations, the resulting WLS-SE problem is often solved using some variation of the Gauss-Newton method. A common candidate for solving nonlinear least-squares problems, the Gauss-Newton algorithm is rooted in taking linear approximations in an iterative manner. Challenged by the nonconvex objective, such iterative procedures get stuck at local minima, encounter convergence issues, or experience sensitivity to the initial guess. These issues are often worsened in DSSE solvers due to the aforementioned problems related to ill-conditioned power flow Jacobian matrices.

To address these convergence issues, several reformulations based on different variables and coordinates were considered when SE methods were first

developed specifically for distribution systems. Transmission SE typically relates power measurements to complex voltage in polar coordinates. In [6, 7], power measurements are first converted to equivalent line current measurements while the voltage phasors are represented in rectangular coordinates. These current-based formulations capitalize on the fact that the resulting gain matrix is constant. Hence, the computation needed to build and factorize the gain matrix is simplified and the algorithm time can be greatly reduced. Despite accelerated computation, these methods may likely converge to a local optimum in the presence of a large number of more accurate measurements of current magnitude. Furthermore, the computational benefits associated with the constant gain matrix will diminish for meshed distribution systems. In [8,9], the DSSE can be formulated using branch currents in rectangular or polar coordinates as the system states, instead of the voltages. This transformation is more powerful, decoupling the system into per-phase analysis, which would lead to smaller subproblems for each phase. Yet this method is still sensitive to disproportional weighting factors arising from variations in measurement accuracy, while the initialization again plays a crucial role in the update trajectory.

In addition to the aforementioned numerical issues, the lack of accurate or real-time measurements also challenges DSSE with system observability issues. Although more and more sensing and communication infrastructure have been deployed to distribution networks, the level of measurement redundancy still lacks in comparison with transmission networks. Hence, it is imperative for the SE to include all available network and load information. Traditional metered measurements for DSSE include real and reactive power flows and injections, voltage magnitudes, and sometimes current magnitudes. In addition to these, DSSE have to also incorporate the following:

- pseudomeasurements
- virtual measurements
- μPMU data

Pseudomeasurements typically refer to load forecasts obtained from historical data. They may be necessary to achieve system observability, but they can be viewed as less accurate "measurements" compared to metered data,

thus the much higher noise variance level. Accordingly, the noise standard deviation of pseudomeasurements could be dozens of times that of metered measurements.

As for virtual measurements, they correspond to network constraints at zero-injection nodes. Typically at switching devices or branching nodes, there is no load or generation, and thus the complex power injection exactly equals zero. This more commonly exists in distribution systems than transmission ones. One approach to including such constraints into the iterative DSSE solvers is to treat them as slightly noisy data at extremely high fidelity. Essentially, a much larger weight would be given to the virtual measurements in the WLS error objective. In the presence of both virtual measurements and pseudomeasurements, there exists a high level of variation among the accuracy of all input information. Accordingly, the conditioning of the gain matrix obtained by iterative linearization would degrade. Another approach is to incorporate zero-injection bus data using Lagrange multipliers [7]. The system of equations resulting from the problem's necessary conditions can be solved iteratively by Gauss-Newton as well. The challenge is that the resulting system of equations is not only larger than the original unconstrained one, but also indefinite, requiring specialized factorization techniques to ensure numeric stability.

Micro-phasor measurement unit (μPMU) data is becoming more available in distribution systems along with the development of synchrophasor technology in transmission grid monitoring. Phasor measurement units (PMUs) are increasingly employed to provide high-resolution and synchronized samples of voltage and current phasors. For economic and technical concerns, a more cost-effective counterpart, the μPMU device, has been advocated for distribution system monitoring [10]. A number of linear SEs have been developed using synchrophasor measurements, including [11–14]. However, these efforts are limited by an inability to include any other type of data, preventing their widespread adoption. Because of the small number of μPMU devices deployed currently and in the near future, it is crucial for any practical DSSE solver to incorporate both traditional and new data types in a hybrid fashion [15, 16].

Recent research efforts in DSSE have focused on either real system implementation challenges [17–23], or extending the problem to include objectives such as meter placement and distributed generation control [24–28] . By and

large, these methods still rely on iterative update procedures by linearizing the multi-phase relationship between power and voltage phasors. Although existing infrastructure and algorithm developments have significantly advanced monitoring capabilities in distribution networks, DSSE solvers are still challenged by two main issues. First, the unbalanced multi-phase power flow model leads to higher computational complexity in the linearization step. Second, the algorithmic core of iterative updates adopted by existing solvers fails to address the numerical conditioning issues, especially considering the vast differences in measurement accuracy. Therefore, it is of high interest to develop new DSSE algorithms that address these shortcomings and achieve the dual objectives of efficiency and robustness.

1.2 Thesis Contributions and Outline

This thesis aims to develop efficient and robust DSSE approaches that can resolve the divergence issues of existing solvers and incorporate all relevant data and information regarding the system and its loads. Our DSSE algorithms are proposed by considering two classes of multi-phase power flow modeling approaches that are different from the existing relations between power and voltage phasors. Specifically, the first DSSE method builds upon reformulating the problem as a semidefinite programming (SDP) problem to solve for a matrix system state inspired by the quadratic relationship between power and voltage quantities. The second DSSE method utilizes a linear power flow model, relating power and voltage magnitude quantities, to enable more efficient computation.

In contrast to the potential convergence issues encountered using standard power flow modeling and iterative solvers, problems cast as SDPs have desirable performance characteristics and can even attain the global optimum in polynomial-time. SDP has been of recent interest in several power system applications, including transmission system SE [29] and the optimal power flow problem for distribution systems [30]. In this thesis, a DSSE solver is proposed, founded on a reformulation of the power flow model which takes advantage of the naturally linear relationship between power and voltage squared and a relaxation of the rank constraint. This yields a convex SDP problem which can be efficiently solved by interior-point methods, but also

easily incorporate virtual measurement equality constraints. Without concern for convergence to a local optimum or lack of convergence thereof, satisfactory approximation of the original nonconvex SE problem is expected and demonstrated. Due to time complexity, SDP may not be appropriate for large-scale systems, but does provide a good initialization if there is no prior knowledge of the system.

To eliminate the need for troublesome iterative methods, linear power flow models can also be employed. Akin to the usage of the DC power flow model in transmission systems, a linear, but less accurate, model enables the fast and robust analysis of large systems. The linearized DistFlow (LDF) model [31] was a pioneer of linearized distribution system power flow models, developed to enable system operations and planning. Motivated by the influx of interest in distribution networks, alternatives including a fixed-point based method [32], a rectangular-coordinate formulation [33], and multi-phase unbalanced models [30, 34, 35] have been recently developed. In this thesis, the LDF model is improved upon by introducing a per-phase line flow difference term to counter the error introduced by the minimal loss assumption that enables the linearization. Upon this linearized model, a DSSE problem is formulated by minimizing the weighted measurement mismatch error while adhering to the zero-injection bus equality constraints. The resultant DSSE is a quadratic optimization problem with linear constraints, for which efficient convex optimization solvers are available as well as a closed form solution. The LDF-based formulation is extended to include synchrophasor measurements from μPMUs and the modeling of tap-changing voltage regulators. The proposed LDF-based SE achieves an improved state estimate due to the inclusion of the approximate line flow difference terms and exhibits excellent numerical performance, even for a diverse set of measurements.

This thesis is organized as follows: Chapter 2 develops a multi-phase network model for use with semidefinite programming for distribution system SE. Chapter 3 proposes improvements and extensions to the linearized DistFlow power flow model and formulates an SE method that utilizes the linearity of the model to maintain computational tractability. Chapter 4 provides simulation results for the proposed SE methods on the IEEE 13-bus and 123-bus systems. Chapter 5 summarizes the thesis, highlighting the key modeling, computational, and performance benefits of the two methods and describing intended future work.

CHAPTER 2

SEMIDEFINITE PROGRAMMING FOR DSSE

This chapter will introduce a matrix-based multi-phase network model, formulated to be linear with respect to the outer product matrix of the voltage phasor vector. A least squares-based state estimation problem is developed around this model, and a semidefinite relaxation is applied, rendering the problem a convex SDP with desirable convergence and solution characteristics. This chapter also addresses recovering the voltage vector state from the outer product matrix and a process for bad data detection.

2.1 Matrix Representation for Multi-Phase Power Flow

Consider a distribution network modeled by the graph $\mathcal{G} := (\mathcal{N}, \mathcal{E})$, and let $\mathcal{N} := \{0, ..., N\}$ be the set of nodes connected by line segments in the set $\mathcal{E} := \{(i, j)\} \subset \mathcal{N} \times \mathcal{N}$. Each bus in the system may have one, two, or three phases, each of which corresponds to a node in the set $\mathcal{N}$. Let $\mathbf{v} \in \mathbb{C}^{N\times 1}$ be the complex node voltage vector and let $\mathbf{i} \in \mathbb{C}^{N\times 1}$ be the node current injection vector. The network admittance matrix, $\mathbf{Y} \in \mathbb{C}^{N\times N}$, linearly relates the injected currents to node voltage per Kirchhoff's laws; that is, $\mathbf{i} = \mathbf{Yv}$.

Using the classical methods from [36] to derive the admittance matrix for an unbalanced three-phase system, the resulting matrix contains information about the effects of mutual coupling and branch admittances. The approaches outlined in [36, Ch. 6,8] generalize this modeling for any line segment or component, such as switches, voltage regulators, and transformers. The shunt admittance of a distribution line is often small enough to be ignored without loss of accuracy, though exceptions exist.

The complex power injected at node j can be expressed as

$$p_j + \mathbb{j}q_j = v_j I_j^* = v_j \sum_{k=1}^{n} (Y_{jk} v_k)^* \tag{2.1}$$

where Y_{jk} is the (j,k)-th entry of $\mathbf{Y}$. Since all elements of $\mathbf{i}$ are linear combinations of v_j's, the nodal complex power $\mathbf{p}_j + \mathbb{j}\mathbf{q}_j$ is quadratic (not linear) with respect to $\mathbf{v}$. Consider expressing the quadratic components linearly in terms of the outer matrix $\mathbf{V} = \mathbf{v}\mathbf{v}^{\mathcal{H}}$. Because of its special structure, matrix $\mathbf{V}$ is positive semidefinite; i.e., $\mathbf{V} \succeq \mathbf{0}$ and rank 1. To develop the linear relation between matrix $\mathbf{V}$ and the complex power injections, define vector $\mathbf{e}_j$ to be all zeros except for the j^{th} entry which will be 1. We define the admittance-related matrix $\mathbf{Y}_j := \mathbf{e}_j\mathbf{e}_j^T\mathbf{Y}$ and build the following matrices:

$$\mathbf{H}_{p,j} := \frac{1}{2}(\mathbf{Y}_j + \mathbf{Y}_j^{\mathcal{H}}) \tag{2.2a}$$

$$\mathbf{H}_{q,j} := \frac{\mathbb{j}}{2}(\mathbf{Y}_j - \mathbf{Y}_j^{\mathcal{H}}) \tag{2.2b}$$

$$\mathbf{H}_{V,j} := \mathbf{e}_j\mathbf{e}_j^T. \tag{2.2c}$$

Using these definitions, the linear formulation of the nodal power with respect to $\mathbf{V}$ becomes

$$p_j = tr(\mathbf{H}_{p,j}\mathbf{V}) \tag{2.3a}$$

$$q_j = tr(\mathbf{H}_{q,j}\mathbf{V}) \tag{2.3b}$$

$$|V_j|^2 = tr(\mathbf{H}_{V,j}\mathbf{V}) \tag{2.3c}$$

where tr denotes the matrix trace operator.

2.2 SDP-based State Estimation

The purpose of state estimation is to obtain the unknown voltage magnitudes and angles from a set of measurements that may include the following quantities:

- $|V_j|$: the voltage magnitude at node j;
- P_j: the real power injected at node j;
- Q_j: the reactive power injected at node j.

In practice, metered measurements are known to be corrupted by noise. The general measurement model for the i-th measurement can be described by

$$z_i = h_i(\mathbf{v}) + \epsilon_i \tag{2.4}$$

where $h_i(\mathbf{v})$ denotes the corresponding measurement function for each z_i. Additive measurement noise ϵ_i is concatenated into a column vector $\boldsymbol{\epsilon}$, where each $\epsilon_i \sim \mathcal{N}(0, \sigma_i^2)$ is Gaussian distributed and independent. The set of metered power injection and voltage magnitude measurements constitute the vector $\mathbf{z} = (z_1, z_2, ..., z_m)^T$, where entries $z_1, ..., z_m$ can be metered measurements, pseudomeasurements estimated from historical data, or a combination thereof. The set of nonlinear functions $h(\mathbf{v})$ represents the physical relationship between $\mathbf{z}$, $\mathbf{v}$, and ϵ.

The goal of SE is to find an estimate of $\mathbf{v}$, denoted by $\hat{\mathbf{v}}$, that best matches the measurement set $\mathbf{z}$ according to the relationships in (2.4). To that end, a semidefinite relaxation (SDR) approach to DSSE is considered. Since (2.3) provides a linear relationship between the measurement values and $\mathbf{V}$, as opposed to the quadratic relationship in (2.1), let $\mathbf{H}_i$ denote the corresponding measurement matrix for each z_i. Desiring to minimize the difference between the measured and estimated data leads to the following WLS estimator:

$$\begin{aligned} \hat{\mathbf{V}} = \arg\min_{\mathbf{V} \in \mathbb{C}^{n \times n}} & \sum_{i=1}^{m} \frac{1}{\sigma_i^2} \Big[z_i - tr(\mathbf{H}_i \mathbf{V}) \Big]^2 \\ \text{s.t. } & tr(\mathbf{H}_i \mathbf{V}) = 0, i = m+1, ..., m+l \\ & \mathbf{V} \succeq \mathbf{0}, \text{and rank}(\mathbf{V}) = 1. \end{aligned} \tag{2.5}$$

The objective captures the minimization of the difference between the measured ($i = 1, ..., m$) and estimated data, while the virtual measurements ($i = m+1, ...m+l$) are accounted for in the equality constraints. The constraints on matrix $\mathbf{V}$ are a result of the structure of the outer product matrix.

Although z_i and $\mathbf{V}$ are linearly related, the reformulated problem (2.5) is still nonconvex. The rank constraint of $\mathbf{V}$ is the cause of this nonconvexity. To address this, the rank constraint is relaxed, and (2.5) is converted to a standard SDP problem formulation. By Schur's complement lemma [29], the quadratic objective of (2.5) can be represented by a linear weighted cost by

introducing an auxiliary vector $\boldsymbol{\chi} \in \mathbb{R}^m$, as given by

$$\begin{aligned}
\{\hat{\mathbf{V}}, \hat{\boldsymbol{\chi}}\} = \underset{\mathbf{V}, \boldsymbol{\chi}}{\operatorname{argmin}} \ & \mathbf{w}^T \boldsymbol{\chi} \\
\text{s.t.} \ & \begin{bmatrix} \chi_i & z_i - tr(\mathbf{H}_i \mathbf{V}) \\ z_i - tr(\mathbf{H}_i \mathbf{V}) & 1 \end{bmatrix} \succeq \mathbf{0}, i = 1, ..., m \\
& tr(\mathbf{H}_i \mathbf{V}) = 0, i = m+1, ..., m+l \\
& \mathbf{V} \succeq \mathbf{0}
\end{aligned} \tag{2.6}$$

where the weight vector $\mathbf{w} = [\frac{1}{\sigma_1^2}, ..., \frac{1}{\sigma_m^2}]^T$.

This reformulated SE problem (2.6) is now in the standard convex SDP form. Hence, it can be efficiently solved using convex optimization solvers. The performance will be verified numerically in Section 4.1. Notably, the SDP-based SE formulation incorporates the zero-injection virtual measurements using equality constraints. Due to the convexity of (2.6), the highly accurate virtual measurements will cause minimal numerical issues, as compared to using the iterative approach for solving the standard problem.

The SDP-based SE formulation can conveniently incorporate additional measurement types, which is especially valuable in networks with minimal measurement redundancy. Line current magnitude data is commonly available in many distribution feeders, often from protection devices. The line current magnitude squared $|I_{jk}|^2$ is also quadratic with respect to $\mathbf{v}$, and hence can be linearly related to $\mathbf{V}$ as in (2.3). The difficulty for including μPMU data in this framework is that the data is linear with respect to the state $\mathbf{v}$. The implementation of such measurements is not covered in this work, but the potential is promising as PMUs have been successfully incorporated into SDP-based SE for transmission systems in [29].

Having recovered $\mathbf{V}$ from the SDP solution, it remains to recover the system state $\mathbf{v}$. To do so, there must exist a one-to-one mapping between the state vector $\mathbf{v}$ and the state matrix $\mathbf{V}$. To prove this, let $\mathbf{v} \in \mathbb{C}^{n \times 1}$. The state matrix $\mathbf{V}$ was defined to be $\mathbf{v}\mathbf{v}^{\mathcal{H}}$, which implies that for every $\mathbf{v}$ there is only one $\mathbf{V}$. Recall that $\mathbf{V}$ is positive semidefinite, symmetric, and rank one; by the spectrum decomposition theorem $\mathbf{V}$ has one unique eigenvalue and eigenvector pair. Therefore, there exists only one $\mathbf{v} = \sqrt{\lambda_1}\mathbf{g_1}$ such that $\mathbf{v}\mathbf{v}^{\mathcal{H}}$ for every $\mathbf{V}$. This shows that there is a one-to-one mapping between $\mathbf{v}$ and $\mathbf{V}$.

The SDP solution $\hat{\mathbf{V}}$ procured from (2.6) is only approximately rank-one because of the semidefinite relaxation and subsequent removal of the rank-one constraint in (2.6). One way to recover the state $\mathbf{v}$ is by using the largest eigenvalue. Applying eigenvalue decomposition gives

$$\hat{\mathbf{V}} = \sum_{i=1}^{\rho} \lambda_i \mathbf{g_i} \mathbf{g}_i^{\mathcal{H}} \tag{2.7}$$

where ρ is the rank of matrix $\hat{\mathbf{V}}$, $\lambda_1 \geq \lambda_2 \geq ... \geq \lambda_p \geq 0$ are the eigenvalues of matrix $\hat{\mathbf{V}}$, and $\mathbf{g}_1, \mathbf{g}_2, ...\mathbf{g}_p$ are the corresponding eigenvectors. Since $\lambda_1 \mathbf{g_1} \mathbf{g}_1^{\mathcal{H}}$ is the best rank-one approximation to $\mathbf{V}$, the SDP-based SE is $\hat{\mathbf{v}} = \sqrt{\lambda_1}\mathbf{g}_1$.

Lastly, it is advantageous to consider bad data detection for robust SE problems [3]. The weighted least absolute value (WLAV) error criterion is known to handle outliers when there is sufficient measurement redundancy. One method by which to detect bad data is to obtain the SE from a WLAV estimator and check the residuals. A residual with large magnitude is a likely candidate for bad data.

2.3 Chapter Summary

In this chapter, a state estimation method is developed using a matrix-based representation of the multi-phase power flow equations and semidefinite programming. First, the power flow measurements are uniquely reformulated to be linear in the outer product matrix, $\mathbf{V}$. Then the SDP SE problem is introduced and relaxed, enabling computationally efficient solvers to achieve the global optimum. A different power flow model and solution method distinguish this formulation from existing DSSE methods.

CHAPTER 3

LINEAR POWER FLOW MODELING FOR DSSE

This chapter provides an introduction to linearized power flow models for distribution systems. Linear power flow models have computational and numeric stability benefits when used in the state estimation problem. The LinDistFlow based models for single-phase networks are first introduced, then extended to their multi-phase counterparts. Both models are written in matrix form to emphasize their linear form. The resulting power flow solutions are compared with those provided by alternative linear power flow models of recent interest. The methods developed in this chapter are then incorporated into efficient and robust state estimators for distribution systems.

3.1 Modeling of Single- and Multi-Phase Networks

The methods proposed in this work are a variant of the DistFlow method formulated in [31]. Consider a distribution network modeled by the graph $\mathcal{G} := (\mathcal{N}, \mathcal{E})$, and let $\mathcal{N} := \{0, ..., N\}$ be the set of buses connected by line segments in the set $\mathcal{E} := \{(i,j)\} \subset \mathcal{N} \times \mathcal{N}$. For each line (i,j), let $z_{ij} = r_{ij} + \mathbb{j}x_{ij}$ denote the complex impedance and

$$S_{ij} = P_{ij} + \mathbb{j}Q_{ij} \tag{3.1}$$

the complex line flow from bus i to j. Additionally, let v_j, p_j, and q_j be the voltage magnitude, real and reactive power injection, respectively, per bus j. All quantities are in per unit (p.u.). Figure 3.1 is an example of a distribution network labeled accordingly. The power flow and voltage drop for line (i,j) is modeled by the DistFlow equations [31]:

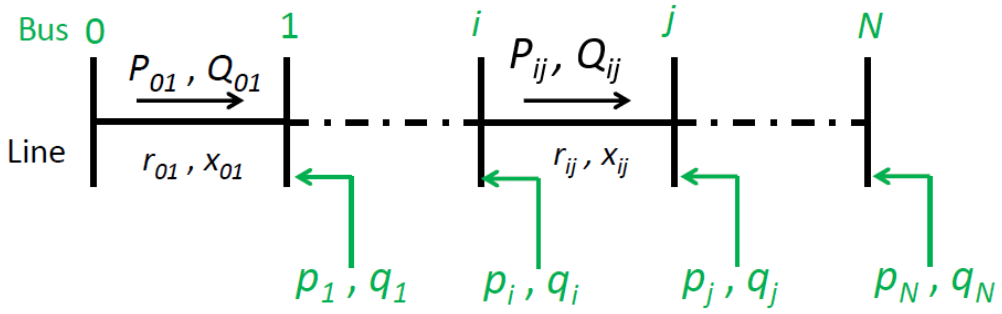

Figure 3.1: An example of a radial feeder

$$P_{ij} - \sum_{k \in \mathcal{N}_j^+} P_{jk} = -p_j + r_{ij} \frac{P_{ij}^2 + Q_{ij}^2}{v_i^2} \tag{3.2a}$$

$$Q_{ij} - \sum_{k \in \mathcal{N}_j^+} Q_{jk} = -q_j + x_{ij} \frac{P_{ij}^2 + Q_{ij}^2}{v_i^2} \tag{3.2b}$$

$$v_i^2 - v_j^2 = 2(r_{ij} P_{ij} + x_{ij} Q_{ij}) - (r_{ij}^2 + x_{ij}^2) \frac{P_{ij}^2 + Q_{ij}^2}{v_i^2} \tag{3.2c}$$

where $\mathcal{N}_j^+ = \{k | (j,k) \in \mathcal{E} \text{ with } k \text{ downstream from } j\}$. The fractional term $(P_{ij}^2 + Q_{ij}^2)/v_i^2$ is equivalent to the squared current magnitude for line (i,j), and contributes to the line power loss terms in equations (3.2a)- (3.2b). Assuming negligible line flow losses, define

$$\mu_i := v_i^2. \tag{3.3}$$

Then (3.2) can be approximated by the LinDistFlow (LDF) equations [31] as follows:

$$P_{ij} - \sum_{k \in \mathcal{N}_j^+} P_{jk} = -p_j \tag{3.4a}$$

$$Q_{ij} - \sum_{k \in \mathcal{N}_j^+} Q_{jk} = -q_j \tag{3.4b}$$

$$\mu_i - \mu_j = 2(r_{ij} P_{ij} + x_{ij} Q_{ij}). \tag{3.4c}$$

In [31], a Taylor series expansion is performed to transform (3.4c) to a linear function of v_i. The proposed method maintains the linearity in v_i^2 to avoid the

loss in accuracy from an additional assumption at the minimal computational cost of taking the square root of the elements of the solution vector.

To illustrate the linearity of (3.4), a matrix representation is introduced. Let $\mathbf{M}^0$ denote the $(N+1) \times N$ graph incidence matrix for network $\mathcal{G}$. For each line segment $(i,j) \in \mathcal{E}$, set $M^0_{il} = 1$ and $M^0_{jl} = -1$, if bus i is closer to bus 0 than bus j. Then define the vector $\mathbf{m}_0^T$ and the $N \times N$ matrix $\mathbf{M}$ such that $\mathbf{M}^0 = [\mathbf{m}_0 \ \mathbf{M}^T]^T$. Stacking all quantities into vectors, the LDF equations are equivalent to

$$\textbf{LDF:} \qquad \mathbf{MP} = \mathbf{p} \tag{3.5a}$$

$$\mathbf{MQ} = \mathbf{q} \tag{3.5b}$$

$$\mathbf{M}^T\boldsymbol{\mu} + \mathbf{m}_0 = 2(\mathbf{D}_r\mathbf{P} + \mathbf{D}_x\mathbf{Q}) \tag{3.5c}$$

where $\mathbf{D}_r$ is an $N \times N$ diagonal matrix with entries corresponding to line resistance. Similarly $\mathbf{D}_x$ is an $N \times N$ diagonal matrix with entries corresponding to line reactance.

The source of approximation error for the LDF method is the assumption that line flow losses are negligible. A new term is introduced to mitigate the approximation error of (3.5) associated with the ignored fractional loss term. First a power flow solution must be obtained using (3.5); then an adjustment term can be introduced for each line (i,j), denoted by

$$l_{ij} := (P_{ij}^2 + Q_{ij}^2)/\mu_i. \tag{3.6}$$

For each line, estimate the line current terms $\{l_{ij}\}$ and substitute them into (3.2a)-(3.2b) as constant values to form the following model:

$$\textbf{l-LDF:} \qquad \mathbf{MP'} = \mathbf{p} + \mathbf{D}_r\mathbf{l} \tag{3.7a}$$

$$\mathbf{MQ'} = \mathbf{q} + \mathbf{D}_x\mathbf{l} \tag{3.7b}$$

$$\mathbf{M}^T\boldsymbol{\mu'} + \mathbf{m}_0 = 2(\mathbf{D}_r\mathbf{P'} + \mathbf{D}_x\mathbf{Q'}). \tag{3.7c}$$

Linearity of the l-LDF model is maintained because $\mathbf{l}$ is constant, by design. The inclusion of this loss term improves the accuracy of the power flow solution $(\boldsymbol{\mu'}, \mathbf{P'}, \mathbf{Q'})$, as will be shown in the following section.

In addition to the single-phase model, it is imperative to explore a multi-phase model as well because of the unbalanced nature of distribution sys-

tems. Therefore this section will extend the multi-phase LDF model in [37]. An improved approximation using constant adjustment terms similar to the method developed in the previous section for l-LDF is now introduced.

Without loss of generality, assume every bus includes three phases $\{a, b, c\}$. Each phase at each bus is referred to as a node. To account for the mutual coupling effects between phases, the impedance of line (i, j) is represented by the 3×3 matrix $\mathbf{Z}_{ij}$. Accordingly, each bus voltage phasor is denoted by a 3×1 complex vector $\mathbf{V}_j := [V_j^a, V_j^b, V_j^c]^T$. Multiphase Ohm's law states that

$$\mathbf{V}_i = \mathbf{V}_j + \mathbf{Z}_{ij}\mathbf{I}_{ij} \tag{3.8}$$

where $\mathbf{I}_{ij}$ is the 3×1 complex line current vector. The power flow equations (3.5a)-(3.5b) can be readily extended to model multi-phase systems by first collecting all the per-phase line flows and node injections in corresponding vectors. The matrix $\mathbf{M}$ also needs to be modified to maintain the flow conservation at every node.

To obtain the voltage drop relation for line (i, j), multiply each side of multi-phase Ohm's law by its Hermitian conjugate and keep the real-valued diagonal:

$$\text{diag}(\mathbf{V}_i\mathbf{V}_i^{\mathcal{H}}) = \text{diag}(\mathbf{V}_j\mathbf{V}_j^{\mathcal{H}}) + 2\text{Re}\{\text{diag}(\mathbf{V}_i\mathbf{I}_{ij}^{\mathcal{H}}\mathbf{Z}_{ij}^{\mathcal{H}})\} + \text{diag}(\mathbf{Z}_{ij}\mathbf{I}_{ij}\mathbf{I}_{ij}^{\mathcal{H}}\mathbf{Z}_{ij}^{\mathcal{H}}) \tag{3.9}$$

Neglecting the last term which is related to line losses, as was done with the single-phase model, the second term can be approximated by linear combinations of line flows by assuming that the bus voltages are nearly balanced; i.e.,

$$\frac{v_i^a}{v_i^b} \approx \frac{v_i^b}{v_i^c} \approx \frac{v_i^c}{v_i^a} \approx \phi \tag{3.10}$$

where $\phi = e^{\mathrm{j}2\pi/3}$ and $\boldsymbol{\phi} := [1\ \phi\ \phi^2]^T$. The squared voltage $\boldsymbol{\mu}_i := \text{diag}(\mathbf{V}_i\mathbf{V}_i^{\mathcal{H}})$, and (3.9) can be approximated by

$$\boldsymbol{\mu}_i - \boldsymbol{\mu}_j \approx 2\text{Re}\{\tilde{\mathbf{Z}}_{ij}\mathbf{S}_{ij}\} \tag{3.11}$$

where $\mathbf{S}_{ij} = \text{diag}(\mathbf{V}_i\mathbf{I}_{ij}^{\mathcal{H}})$ is the complex line flow and $\tilde{\mathbf{Z}}_{ij} := \text{diag}(\boldsymbol{\phi})\mathbf{Z}_{ij}^{\mathcal{H}}\text{diag}(\boldsymbol{\phi}^*)$

The matrix form of the multi-phase LDF model (m-LDF) is given by

$$\textbf{m-LDF:} \qquad \mathbf{MP} = \mathbf{p} \tag{3.12a}$$

$$\mathbf{MQ} = \mathbf{q} \tag{3.12b}$$

$$\mathbf{M}^T\boldsymbol{\mu} + \mathbf{m}_0 = 2(\mathbf{D}_r\mathbf{P} + \mathbf{D}_x\mathbf{Q}) \tag{3.12c}$$

where $\mathbf{D}_r$ and $\mathbf{D}_x$ are modified to account for the mutual coupling effect; i.e., they are no longer diagonal matrices. They are constructed from linear combinations of the real and reactive parts of $\tilde{\mathbf{Z}}_{ij}$, respectively [37].

As seen in (3.5), the main source of error is due to the approximation of flow conservation. Recall that for the single-phase case, it suffices to use the squared line current to model the difference between the sending and receiving line flows. This no longer holds for multi-phase lines because of mutual coupling and additional losses on the neutral line [36]. The difference between the sending and receiving line flows is defined by

$$\boldsymbol{\Delta}_{ij} := \mathbf{S}_{ij} + \mathbf{S}_{ji} = \mathrm{diag}(\mathbf{Z}_{ij}\mathbf{I}_{ij}\mathbf{I}_{ij}^{\mathcal{H}}) \tag{3.13}$$

by expansion of terms and application of Ohm's law. Substituting the per-phase current in the form $I_{ij}^a = (S_{ij}^a/V_i^a)^*$, the multi-phase line flow difference $\boldsymbol{\Delta}$ as a function of line flows is given by

$$\begin{aligned}
\boldsymbol{\Delta}_{ij} &= \begin{bmatrix} Z_{ij}^{aa}\frac{S_{ij}^{a*}S_{ij}^{a}}{V_i^{a*}V_i^{a}} + Z_{ij}^{ab}\frac{S_{ij}^{b*}S_{ij}^{a}}{V_i^{b*}V_i^{a}} + Z_{ij}^{ac}\frac{S_{ij}^{c*}S_{ij}^{a}}{V_i^{c*}V_i^{a}} \\ Z_{ij}^{ab}\frac{S_{ij}^{a*}S_{ij}^{b}}{V_i^{a*}V_i^{b}} + Z_{ij}^{bb}\frac{S_{ij}^{b*}S_{ij}^{b}}{V_i^{b*}V_i^{b}} + Z_{ij}^{bc}\frac{S_{ij}^{c*}S_{ij}^{b}}{V_i^{c*}V_i^{b}} \\ Z_{ij}^{ac}\frac{S_{ij}^{a*}S_{ij}^{c}}{V_i^{a*}V_i^{c}} + Z_{ij}^{bc}\frac{S_{ij}^{b*}S_{ij}^{c}}{V_i^{b*}V_i^{c}} + Z_{ij}^{ac}\frac{S_{ij}^{c*}S_{ij}^{c}}{V_i^{c*}V_i^{c}} \end{bmatrix} \\
&\approx \begin{bmatrix} Z_{ij}^{aa}S_{ij}^{a*}S_{ij}^{a} & Z_{ij}^{ab}S_{ij}^{b*}S_{ij}^{a}\phi^* & Z_{ij}^{ac}S_{ij}^{c*}S_{ij}^{a}\phi \\ Z_{ij}^{ab}S_{ij}^{a*}S_{ij}^{b}\phi & Z_{ij}^{bb}S_{ij}^{b*}S_{ij}^{b} & Z_{ij}^{bc}S_{ij}^{c*}S_{ij}^{b}\phi^* \\ Z_{ij}^{ac}S_{ij}^{a*}S_{ij}^{c}\phi^* & Z_{ij}^{bc}S_{ij}^{b*}S_{ij}^{c}\phi & Z_{ij}^{ac}S_{ij}^{c*}S_{ij}^{c} \end{bmatrix} \begin{bmatrix} 1/|V_i^a|^2 \\ 1/|V_i^b|^2 \\ 1/|V_i^c|^2 \end{bmatrix}
\end{aligned} \tag{3.14}$$

where the last approximation again assumes nearly balanced voltage. Since $\mu_i = |V_i|^2$, (3.14) can be expressed as

$$\boldsymbol{\Delta}_{ij} = \{\tilde{\mathbf{Z}}_{ij}^{\mathcal{H}} \circ (\mathbf{S}_{ij}\mathbf{S}_{ij}^{\mathcal{H}})\}[\boldsymbol{\mu}_i]^{-1} \tag{3.15}$$

where $\circ$ is the element-wise product operator and $[\bullet]^{-1}$ is the element-wise inverse. Similar to the development of the l-LDF model, $\boldsymbol{\Delta}_{ij}$ can be computed

after obtaining the m-LDF power flow solution to better approximate the flow conservation, leading to the following linear model:

$$\Delta\textbf{-LDF:} \qquad \mathbf{M}\mathbf{P}' = \mathbf{p}' - \mathrm{Re}(\boldsymbol{\Delta}) \tag{3.16a}$$

$$\mathbf{M}\mathbf{Q}' = \mathbf{q}' - \mathrm{Im}(\boldsymbol{\Delta}) \tag{3.16b}$$

$$\mathbf{M}^T\boldsymbol{\mu}' + \mathbf{m}_0 = 2(\mathbf{D}_r\mathbf{P}' + \mathbf{D}_x\mathbf{Q}'). \tag{3.16c}$$

As shown in 3.2, the inclusion of the approximate difference term in the Δ-LDF model improves the accuracy of the power flow solution $(\boldsymbol{\mu}', \mathbf{P}', \mathbf{Q}')$ and maintains the computation benefits of a linear model.

3.2 Comparison of the Linear Models

The proposed models are compared with existing linear alternatives to justify their application to SE. The m-LDF and l-LDF models are first compared with the recently developed linear model using fixed-point approximation (FPA) in [32]. Second, the power flow solution provided by one Newton-Raphson (NR) update using a flat voltage initialization is also compared. Note that the FPA method coincides exactly with the first NR iteration in scenarios with no shunt admittance [33]. These linear methods are tested on a single-phase simplification of the IEEE 123-bus feeder under overloaded conditions, as used in [32]. The MATPOWER [38] power flow program is used to provide the benchmark voltage magnitude profile. Figure 3.2 shows the absolute error in voltage magnitude at each node. The two LDF-based methods outperform the FPA and NR-based methods, including in the overloaded regions (buses 10-35). The further improvement of the l-LDF method is due to the addition of the estimated loss terms.

For multi-phase comparison, the m-LDF and Δ-LDF methods are analyzed against another multi-phase solution achieved by linearizing the power flow manifold [34]. Linearization by the method in [34] after a nonlinear change of coordinates of the state variables is equivalent to the m-LDF model (3.12) under the assumption of zero shunt admittances and using the flat voltage profile as a linearization point. These methods are tested on the IEEE 13-bus feeder [39] case with a fixed voltage regulator tap position to match the published case. The open-source simulator OpenDSS [40] is used to provide

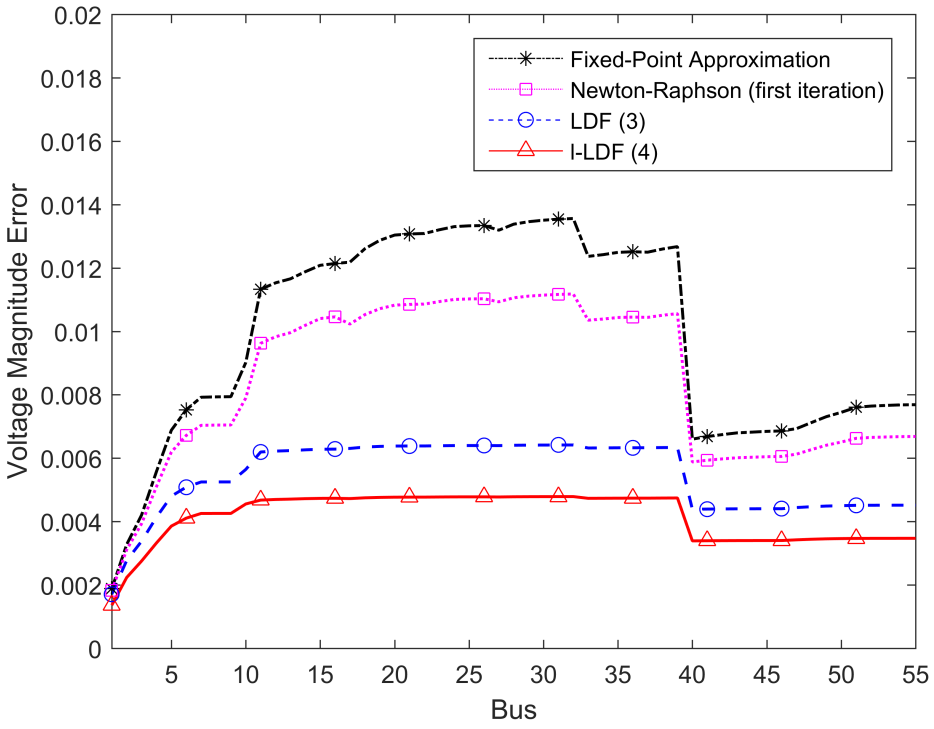

Figure 3.2: Voltage magnitude error of single-phase model for the simplified 123-bus feeder in [32]

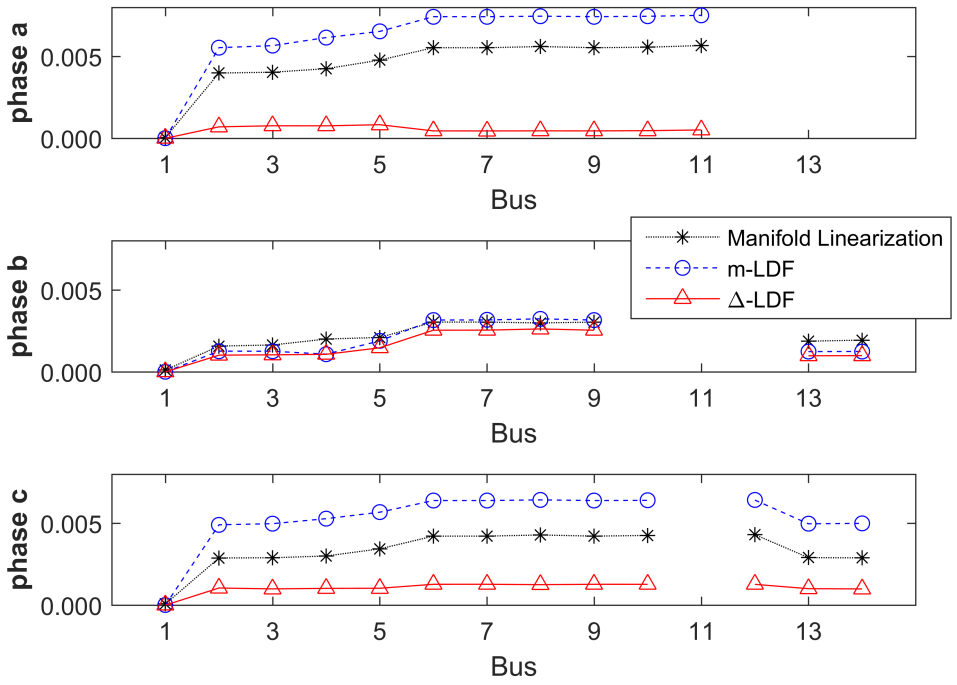

Figure 3.3: Voltage magnitude error of multi-phase model for the IEEE 13-bus feeder

the benchmark three-phase voltage magnitude profile. Figure 3.3 shows the per-phase absolute voltage error at every bus. The Δ-LDF approximation provides the best performance among the three methods, mainly due to the added $\boldsymbol{\Delta}_{ij}$ correction terms in the line flow equations. Without this correction, the other two methods underestimate the line flows and thus do not fully capture the line voltage difference. Unfortunately the error seen near the feeder head can be propagated by the voltage drop equation down the rest of the feeder. These results from the single-phase and multi-phase systems have demonstrated the importance of including the line flow difference term in the linear power flow equations. It was also shown that the LDF-based methods provide competitive accuracy in a computationally reasonable way, suitable for further applications, such as SE.

3.3 LDF-based State Estimation

In this section, the previously introduced class of LDF models are leveraged to develop a fast and accurate SE for distribution systems. The resultant LDF-based SE allows for the integration of diverse data sources such as virtual measurements at zero-injection buses and highly accurate synchrophasor measurements. It will also be extended to include estimation of transformer tap position for voltage regulators.

3.3.1 LDF-Based State Estimation

Define vector $\mathbf{x} := (\boldsymbol{\mu}, \mathbf{P}, \mathbf{Q})$ to be the system state under the LDF models. Because of the linearity of the LDF-based models, all metered measurements are linearly related to the system states, i.e., $\mathbf{z} = \mathbf{H}\mathbf{x} + \boldsymbol{\epsilon}$, with $\boldsymbol{\epsilon} \sim \mathcal{N}(\mathbf{0}, \mathbf{R})$. Incorporating the m-LDF power flow equations into the weighted least squares problem leads to the following problem:

$$\begin{aligned} < \hat{\boldsymbol{\mu}}, \hat{\mathbf{P}}, \hat{\mathbf{Q}} > \; = \; \arg\min_{\mathbf{x}} \quad & \left\| \mathbf{R}^{-\frac{1}{2}} \left[\mathbf{z}_{\mathcal{M}} - \mathbf{H}\mathbf{x} \right] \right\|_2^2 \\ \text{subject to} \quad & \mathbf{M}^T \boldsymbol{\mu} + \mathbf{m}_0 = 2(\mathbf{D}_r \mathbf{P} + \mathbf{D}_x \mathbf{Q}) \\ & \mathbf{M}_{\mathcal{Z}} \mathbf{P} = \mathbf{0} \\ & \mathbf{M}_{\mathcal{Z}} \mathbf{Q} = \mathbf{0} \end{aligned} \tag{3.17}$$

where $\mathbf{M}_{\mathcal{Z}}$ selects the rows of $\mathbf{M}$ that correspond to zero-injection buses. Because the error cost in (3.17) is quadratic, directly incorporating the virtual measurements as linear equality constraints does not affect the convexity of the problem. A variety of convex solvers are available to solve (3.17) efficiently. Indeed it is a linearly constrained quadratic program and thus a closed-form solution exists; see, e.g., [41, 42].

This convex SE problem can be easily extended to incorporate the difference term introduced for the Δ-LDF model. Using the preliminary estimate $(\hat{\boldsymbol{\mu}}, \hat{\mathbf{P}}, \hat{\mathbf{Q}})$ obtained by (3.17), one can calculate the difference term $\boldsymbol{\Delta}$ using (3.15). Now the real power injection measurement modeled is updated as $\mathbf{z}_p = \mathbf{p}_{\mathcal{M}} + \boldsymbol{\epsilon}_p = \mathbf{M}_p \mathbf{P} + \mathrm{Re}(\boldsymbol{\Delta}_p) + \boldsymbol{\epsilon}_p$. This modification can be captured by a constant vector $\mathbf{d}$ added to the linear measurement model for $\mathbf{z}$, and thus

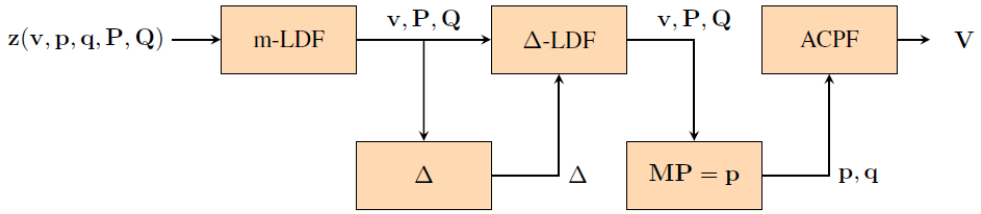

Figure 3.4: Flow chart depicting the steps of the Δ-LDF:AC method

the LDF-based SE model would become

$$\begin{aligned} \underset{\mathbf{x}=(\boldsymbol{\mu},\mathbf{P},\mathbf{Q})}{\text{minimize}} \quad & \left\| \mathbf{R}^{-\frac{1}{2}} \left[\mathbf{z}_{\mathcal{M}} - (\mathbf{H}\mathbf{x} + \mathbf{d}) \right] \right\|_2^2 \\ \text{subject to} \quad & \mathbf{M}^T \boldsymbol{\mu} + \mathbf{m}_0 = 2(\mathbf{D}_r \mathbf{P} + \mathbf{D}_x \mathbf{Q}) \\ & \mathbf{M}_{\mathcal{Z}} \mathbf{P} = -\text{Re}(\boldsymbol{\Delta}_{\mathcal{Z}}) \\ & \mathbf{M}_{\mathcal{Z}} \mathbf{Q} = -\text{Im}(\boldsymbol{\Delta}_{\mathcal{Z}}) \end{aligned} \tag{3.18}$$

where the zero-injection constraints are also updated to reflect the constant difference term. The formulation remains a quadratic optimization problem with linear constraints that can be solved efficiently by available convex solvers or analytically.

As a final step, results from the Δ-LDF method are used to solve the traditional AC power flow (ACPF). The estimated $\mathbf{P}$, $\mathbf{Q}$ and $\boldsymbol{\Delta}$ from the Δ-LDF method are converted to $\mathbf{p}$ and $\mathbf{q}$ and used as inputs for standard AC power flow analysis, as seen in Fig. 3.4. This approach returns the complex voltage phasor everywhere in the system. Hence, although the proposed LDF-SE formulation only includes the magnitude as the unknowns and not the phase angles, it is possible to eventually estimate both as the LDF-SE method can recover the per-phase power flows everywhere in the system. It will henceforth be referred to as the Δ-LDF:AC method in numerical comparisons.

3.3.2 Incorporating Diverse Measurements

The LDF-based SE approaches are now extended to incorporate available μPMU measurements in addition to traditional meter data.

The bus voltage phasor data simply provides voltage magnitude informa-

tion, while line current phasor data along with the bus voltage phasor can be converted to complex power flow measurements. Both of these types of measurements can be directly integrated into the SE formulation in (3.17). By design, they are much more accurate than traditional meter data and should be weighted accordingly. With the ability to monitor multiple lines connected to the same node with high precision, just a few μPMUs can greatly contribute to the model observability and estimation accuracy.

Furthermore, the present SE framework can potentially incorporate the current magnitude measurements available from protection devices. Without the phase angle information as in μPMU data, one needs to assume knowledge of power factor in order to convert these measurements to power flow values. Approximate power factor can be obtained from historic data and the resulting power flow measurements may have lower accuracy than if metered. Fortunately, the proposed SE formulation is robust to high variability of data quality, which makes it suitable for incorporating a multitude of data sources ranging from highly accurate virtual measurements to pseudo-measurements derived from less reliable historic data.

3.3.3 Incorporating Transformer Tap Position

Voltage regulating autotransformers with automatic tap-changing mechanisms are a common component in distribution networks. They are often ignored in literature on DSSE under the assumption of infrequent tap changing actions. Increasing system dynamics and intermittency motivates the consideration of this pervasive component particularly in SE applications [10].

By introducing a virtual secondary-side bus for every regulating transformer as developed in [43],[44], one can obtain an equivalent transformer model that can be incorporated with the m-LDF approximation to estimate voltage regulator tap position. Figure 3.5 shows the original transformer model and the equivalent one. For an ideal transformer t between buses p_t and s_t, a virtual bus s'_t is inserted in between. Equivalently, an ideal transformer connects p_t and s'_t and the bus voltage relationship is given by $V_{p_t} = a_t V_{s'_t}$ where the discrete tap ratio a_t takes one of the 32 values uniformly distributed within a rated range $[\underline{a}, \bar{a}]$. To tackle the nonlinearity

in modeling the line current-bus voltage relationship, the power flow across the ideal transformer is replaced by a pair of additional injections, namely $-S_{p_t s'_t}$ and $S_{p_t s'_t}$, at buses p_t and s'_t, respectively. Buses p_t and s'_t are considered to be physically disconnected, but related by the injection variable $S_{p_t s'_t}$. All system vectors and matrices need to be augmented to include the virtual buses. Accordingly, the augmented matrix $\mathbf{M}$ can still be derived from the incidence matrix, but it is no longer invertible as the graph becomes disconnected by using the equivalent transformer model. The system augmentation introduces additional linear equality constraints, adopted from the ideal transformer relations, given by $\mu_{s'_t} = a_t^2 \mu_{p_t}$, $p_{p_t} = -p_{s'_t}$, and $q_{p_t} = -q_{s'_t}$, for every transformer t. Even though the values that a_t can take are discrete, high granularity of the available positions enables the treatment of the tap ratio as a continuous variable. Accordingly, the tap ratio satisfies $\underline{a}^2 \leq a_t^2 \leq \overline{a}^2$, which can be captured by linear equality constraints to bypass the complexity of having discrete constraints. By combining all the additional constraints associated with the equivalent transformer model, the SE problem can now be updated to

$$
\begin{aligned}
\underset{\mathbf{x}=(\boldsymbol{\mu},\mathbf{P},\mathbf{Q})}{\text{minimize}} \quad & \left\| \mathbf{R}^{-\frac{1}{2}} \left[\mathbf{z}_{\mathcal{M}} - \mathbf{H}\mathbf{x} + \mathbf{d} \right] \right\|_2^2 \\
\text{subject to} \quad & \mathbf{M}^T \boldsymbol{\mu} + \mathbf{m}_0 = 2(\mathbf{D}_r \mathbf{P} + \mathbf{D}_x \mathbf{Q}) \\
& \mathbf{M}_{\mathcal{Z}} \mathbf{P} = -\text{Re}(\boldsymbol{\Delta}_{\mathcal{Z}}) \\
& \mathbf{M}_{\mathcal{Z}} \mathbf{Q} = -\text{Im}(\boldsymbol{\Delta}_{\mathcal{Z}}) \\
& \mathbf{p}_{p_t} = -\mathbf{p}_{s'_t} \quad \mathbf{q}_{p_t} = -\mathbf{q}_{s'_t} \quad \forall t \in \mathcal{T} \\
& \boldsymbol{\mu}_{s'_t} \leq \bar{a}_t^2 \boldsymbol{\mu}_{p_t} \quad \underline{a}_t^2 \boldsymbol{\mu}_{p_t} \leq \boldsymbol{\mu}_{s'_t} \quad \forall t \in \mathcal{T}
\end{aligned}
\tag{3.19}
$$

for the set of voltage regulators $\mathcal{T}$. In this formulation the tap position a_t is not estimated as a state, but it can be recovered by taking the ratio between the estimated $\mu_{s'_t}$ and μ_{p_t}. Recall that vector $\mathbf{m}_0$ in the m-LDF equations is a reference for the system and similar references need to be available for each area of the disconnected graph created by introducing the virtual bus. To provide a reference in each island of the graph, at least one voltage magnitude measurement is required per area, per phase. Again, this problem remains a quadratic problem with linear constraints conveniently solved by available convex solvers.

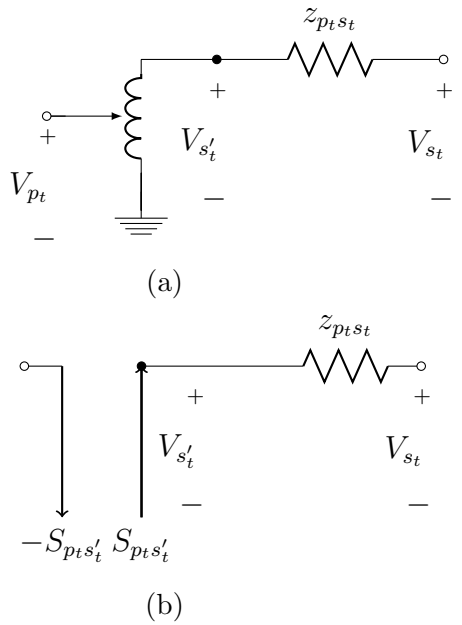

Figure 3.5: Classical transformer model (a), and its equivalent transformer model (b) in [44]

3.4 Chapter Summary

In this chapter, a family of LDF-based state estimators was considered. Improvements were made to the classic LDF formulation by a two-step process where an initial estimate is used to approximate the nonlinear term assumed to be small and ignored in the development of the model. Including this term as a constant in the subsequent estimation improves the solution yet maintains the quadratic form with linear constraints that is efficiently solved by convex solvers. The formulation is extended to include μPMU measurements as inputs and to model transformers such that the tap position can be estimated.

CHAPTER 4

SIMULATION RESULTS

In this chapter, the proposed DSSE methods are demonstrated on various IEEE distribution feeder test cases. These cases include zero-injection buses, which provide the opportunity to exhibit the incorporation of virtual measurements as linear constraints allowed by both formulations. Furthermore, the robustness of the methods is also tested, either through the introduction of bad data or the increase in measurement noise. The system admittance matrix and the complex voltage vector used as the solution reference were procured via the distribution system modeling software OpenDSS [40]. We use the MATLAB-based optimization package CVX [45] with the solver Mosek [46] to solve the SDP and quadratic optimization problems.

4.1 SDP-based State Estimation Results

In this section, the SDP-based state estimation method is applied to a modified IEEE 13-bus distribution feeder system as shown by Fig. 4.1 [39]. This 13-bus network has typical characteristics found in typical distribution systems, such as a tree-like topology, regulators and switches, single-phase and two-phase lines, high R/X ratios, and unbalanced loads.

For this analysis, the distributed load along the line between buses 632 and 671 is modeled by a spot load located a third of the way down the line at a new bus is referred to as Bus 670. The voltage regulator between the feeder source and Bus 632 is removed.

The following measurements are collected for the 13-bus case: real and reactive power injection measurements at load nodes and virtual measurements at zero-injection nodes, which will be incorporated as equality constraints. A key benefit of SDP-based SE is that the solution is not dependent on or sensitive to the initial guess. Furthermore, it is known that an initial guess

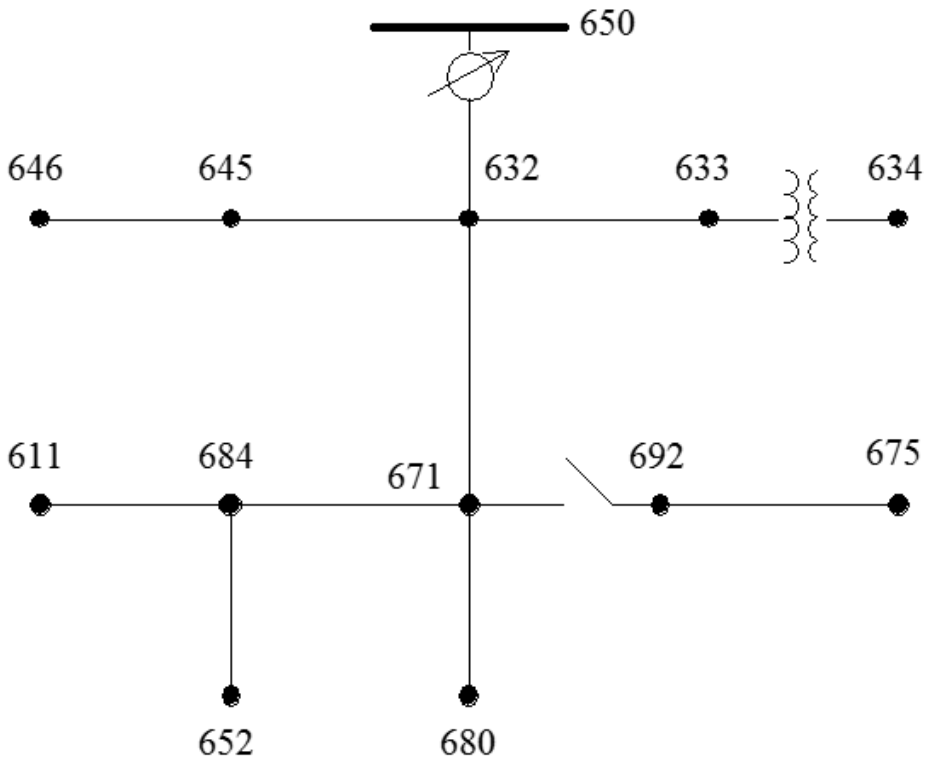

Figure 4.1: The IEEE 13-bus test feeder

near the actual solution can increase the likelihood that the iterative WLS solution will converge to the correct values. Therefore, in addition to the results of using SDP alone, the benefit of using the SDP estimate as an initial guess, which will be referred to as the SDP-WLS approach, is also shown. The estimation error $\|\mathbf{v} - \hat{\mathbf{v}}\|_2$ is averaged over 50 realizations for both approaches. Performance results for the SDP and SDP-WLS estimators are shown in Table 4.1 and Figs. 4.2-4.3.

To demonstrate the robustness of the SDP-based approach, a WLAV estimator is developed for bad data detection. To show proof of concept for

Table 4.1: Euclidean norm estimation error results of the SDP SE scheme for the 13-bus system

	SDP	SDP-WLS
$\|\mathbf{v} - \hat{\mathbf{v}}\|_2$	0.0454	0.0331
Time (sec)	9.080	9.309

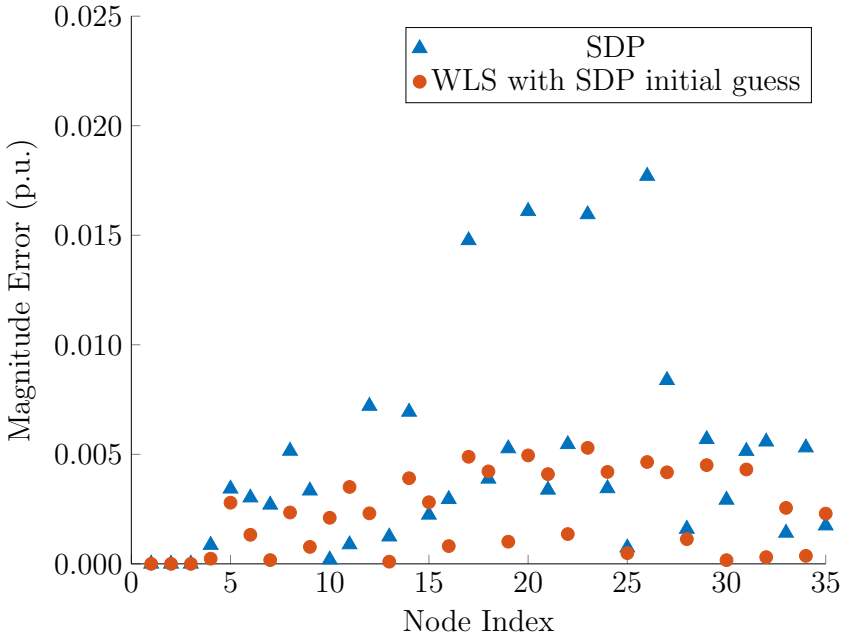

Figure 4.2: SDP estimation error comparison of node voltage magnitude for the 13-bus system

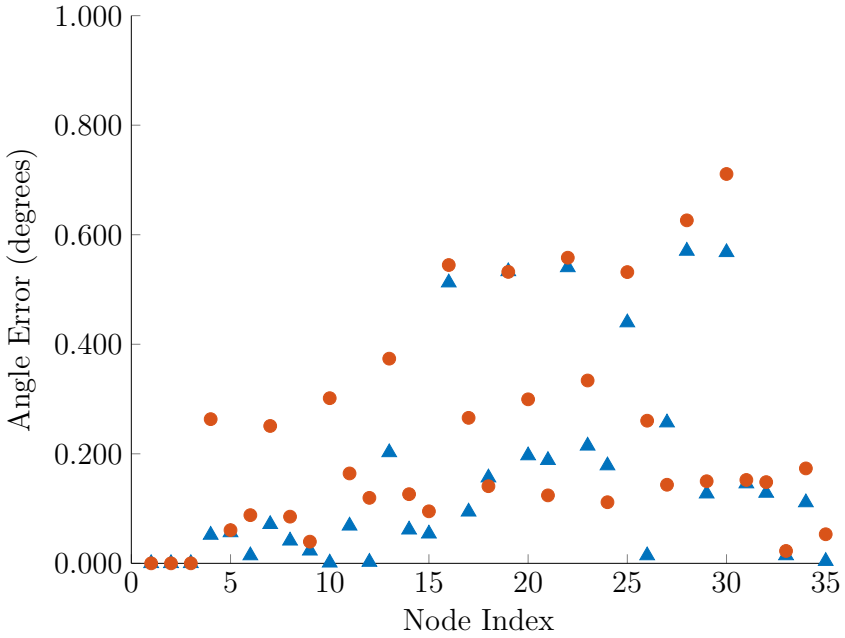

Figure 4.3: SDP estimation error comparison of node voltage angle for the 13-bus system

the SDP-based WLAV approach, measurement redundancy is enhanced by adding voltage magnitude meters. Bad data is generated by randomly picking one measurement from either a power or voltage magnitude meter and

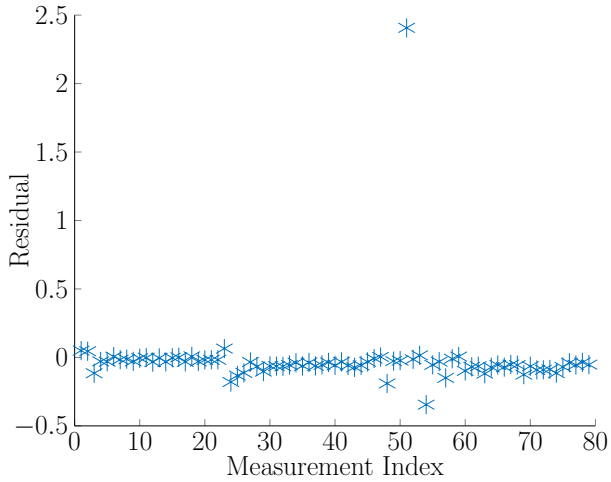

Figure 4.4: Measurement residual at every meter in the 13-bus system for SDP bad data detection

Table 4.2: Euclidean norm estimation error results of the SDP SE scheme for the 13-bus system with bad data

	With Bad Data	With Bad Data Detected/Removed
$\|\mathbf{v} - \hat{\mathbf{v}}\|_2$	0.3524	0.3492

multiplying its value by two. The resulting residual between the measurement value and the reconstructed value is shown in Fig. 4.4 for each meter, which identifies the outlying meter by significantly larger mismatch. After removing this meter, the SDP-WLS estimator is applied using the remaining measurements. Table 4.2 shows that the estimation error performance has been improved after removing the meter data identified as bad based on the residuals. This shows that with sufficient measurement redundancy, the SDP-based WLAV estimator is effective for identifying bad data.

In this section, it was shown that SDP-based SE methods can be a robust and effective alternative to the WLS approach, avoiding local optima and guaranteeing convergence. The most important benefit is that it enables easy incorporation of zero-injection virtual measurements, without potential for convergence or conditioning ill-effects. It also provides a reliable initial guess for a WLS estimator. The SDP formulation for a WLAV bad data detector provides robustness to bad data in cases with sufficient observability. The main drawback to leveraging SDP for SE is the increase in computational time with system size. For example, the run time increase from an average of 2.40 s to 9.08 s as the system size increases from 4 to 13 buses. This

motivates the development of distributed SDP algorithms for SE as seen in [29, 47].

4.2 LDF-based State Estimation Results

In this section, the proposed LDF-based state estimation techniques are tested on the IEEE 13-bus and 123-bus systems [39]. Simulations using LDF-based estimators on the 13-bus and 123-bus system show that solution accuracy can be improved by the inclusion of the Δ term, as seen in the linear model comparison, and μPMU measurements. Also shown are the results of post-processing the estimate using an AC power flow solver, which provides the voltage phasor vector as opposed to the magnitude alone, as produced by standard LDF-based models. Using the 13-bus system, the robustness of the estimator with respect to a diverse set of measurements is shown, by providing results for the inclusion of μPMU measurements as well as pseudomeasurements of varying accuracy and number. The modeling and inclusion of the voltage regulator model is incorporated for the 123-bus system only.

4.2.1 13-Bus Case

For the following tests on the 13-bus system, the available measurements include complex power injection at every load with Gaussian noise $\sigma = 0.02$, virtual measurements at every zero-injection node ($\sigma = 0$), and the three-phase reference voltage at the feeder head. Five SE schemes have been tested: (i) the m-LDF based one in (3.17), (ii) the Δ-LDF based one in (3.18), (iii) the Δ-LDF based scheme with the additional AC power flow step, and (iv,v) the first two schemes with a μPMU installed at Bus 632, a three-phase bus close to the feeder head.

The DSSE performance averaged over 500 random realizations is listed in Table 4.3. The estimator performance metric of root mean square error (rMSE) is given by averaging the voltage magnitude squared error $\sum_j (v_j - \hat{v_j})^2$ over the realizations, and taking its square root. The units of rMSE follow from the corresponding state variables in p.u. In Table 4.3, the Δ-based

Table 4.3: The rMSE results of the four LDF-based SE schemes for the 13-bus system

rMSE	m-LDF	Δ-LDF	Δ-LDF:AC	m-LDF w/ μPMU	Δ-LDF w/ μPMU
v	3.08×10^{-2}	8.65×10^{-3}	5.75×10^{-3}	4.52×10^{-3}	4.18×10^{-3}
P	2.59×10^{-2}	1.45×10^{-2}	1.45×10^{-2}	2.35×10^{-2}	1.30×10^{-2}
Q	6.06×10^{-2}	3.28×10^{-2}	3.28×10^{-2}	3.48×10^{-2}	3.02×10^{-2}

methods provide significant improvement to the real and reactive power flow estimates, with or without μPMU information.

In turn, the voltage magnitude estimate is also improved. For the scheme that also involves acquiring the complex voltage phasor using AC power flow (Δ-LDF:AC), there is an increase in voltage magnitude accuracy in addition to procuring voltage angle information. The per-phase voltage error comparison is depicted in Fig. 4.5 for three of the five schemes. Figure 4.5 supports the claim made in Section 3.2 that the line flow difference terms in the Δ-LDF model increase the SE accuracy. Furthermore, a strategically placed μPMU provides the greatest improvement to the SE schemes, especially in a scenario such as this experiment where our limited measurement set only includes power injection meters.

Our proposed LDF-based SE methods are highly robust to a variety of measurement types and less affected by high variation in measurement accuracy than standard iterative methods. The following simulations show robustness under two conditions: (i) increasing inaccuracy of measurements and (ii) increasing number of inaccurate pseudomeasurements. The first condition to consider is varying the measurement noise level at all load measurements and keeping the zero-injection equality constraints as in the previous tests. At each noise level, the empirical rMSE of the voltage magnitude is averaged over 100 random noise realizations. Figure 4.6 plots the rMSE values for voltage magnitude and real and reactive power flows versus the noise standard deviation of the pseudomeasurements. As is expected, the estimation performance degrades as the pseudomeasurements become more inaccurate, but the estimator still returns a reasonable solution. As the noise level of the pseudomeasurements increases, the improvement of the power flow estimates decreases. This in turn lessens the potential improvement of the voltage magnitude estimates at higher noise levels; this can be seen by comparing the

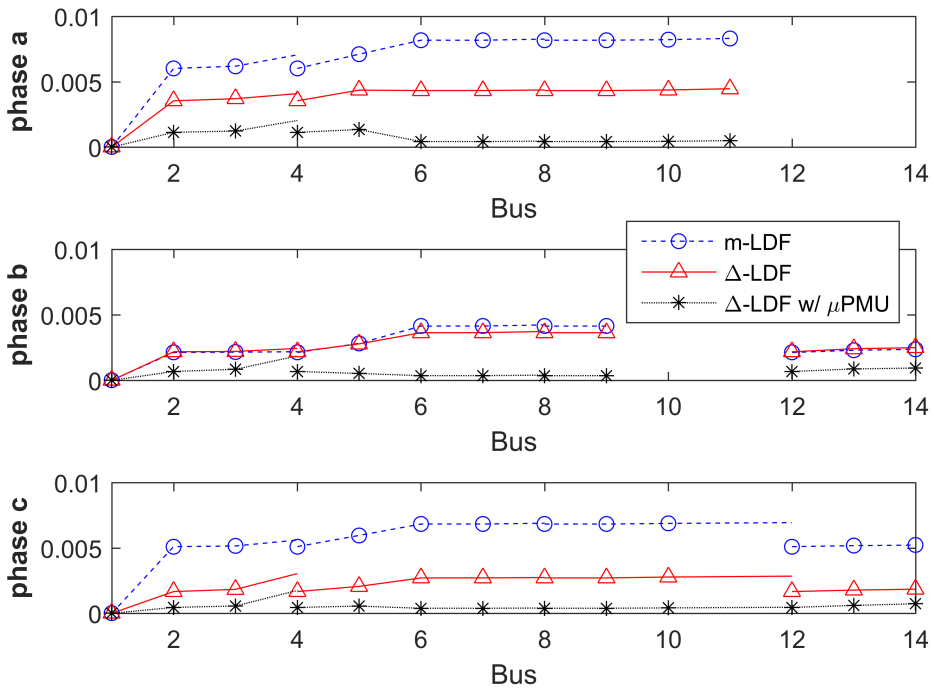

Figure 4.5: Absolute voltage error results of three LDF SE schemes for the 13-bus system

voltage rMSEs of the LDF and Δ-LDF schemes as the noise level increases.

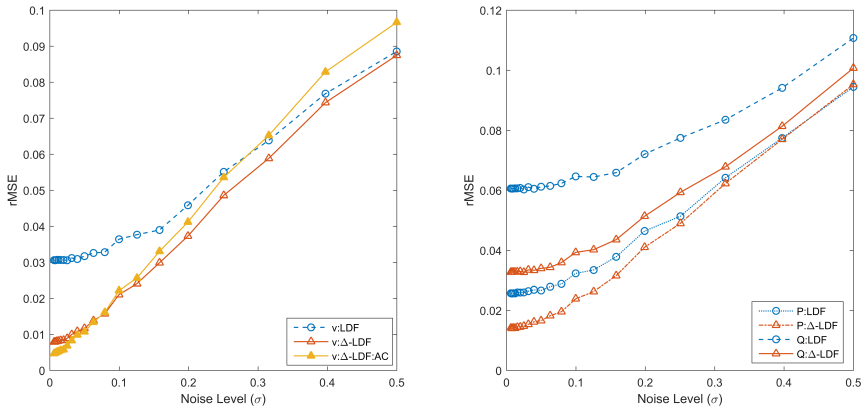

Figure 4.6: Average estimation error in (left) voltage magnitude and (right) line power flows versus the noise level in power injection measurements

To further show the robustness of the proposed LDF-based SE to variations in measurement accuracy, a mix of metered and historically-based measurements is considered. In this test, all metered measurements have $\sigma = 0.02$ and all pseudomeasurements have $\sigma = 0.2$. The number of load nodes chosen to be less accurate pseudomeasurements instead of metered is gradually increased, and the resultant voltage magnitude rMSE over 100 realizations is plotted in Fig. 4.7. The estimation performance is desirable despite the increasing rMSE with an increasing number of pseudomeasurements. This performance degradation seems to be steady, even as the simulation approaches the situation where the estimate is purely based on historical data. Recall that the Δ-LDF:AC method provides voltage magnitude results similar to those of the Δ-LDF model, but it also has the additional output of voltage angle.

These tests on the 13-bus system show that the LDF-based methods provide a family of estimators that easily incorporate a variety of data types without being hampered by the numerical conditioning and convergence issues present in the typical WLS formulations.

4.2.2 123-Bus Case

The 123-bus test feeder case [39] is a radial system with multiple voltage regulators and shunt capacitors. The system contains overhead and under-

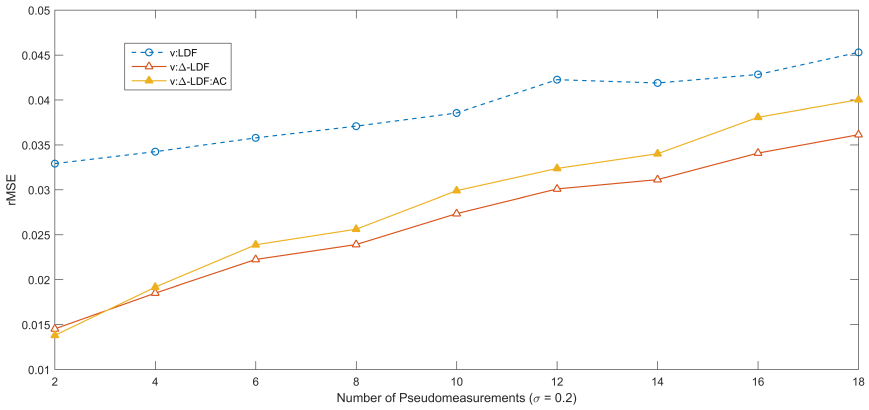

Figure 4.7: Average estimation error in voltage magnitude versus number of measurements (out of 20) chosen to be at a higher noise variance

ground lines, unbalanced loading, and multiple switches. As in the 13-bus tests, power injection measurements are assumed to be available at every load and voltage measurements at a three-phase voltage meter downstream from each voltage regulator. As long as there is a voltage reference in each disconnected graph created by the addition of the virtual secondary bus from the equivalent voltage regulator model, the system will solve. For an initial example, the voltage magnitude errors for the m-LDF and Δ-LDF models are plotted in Fig. 4.8 under noise-free conditions. The data is separated by phase and organized by the nodal distance from the feeder head. Note that the error is significantly higher at phase c. Though not the heaviest loaded phase, its loads, and thereby its line flows, have higher power factor than the other two phases, which seems to affect the accuracy of the model approximation.

In addition to the two SE schemes, m-LDF and Δ-LDF as seen in Fig. 4.8, the first two schemes are simulated with an additional μPMU installed at Bus 14, a three-phase bus near the feeder head that branches into three major feeders. Table 4.4 shows the empirical rMSE for the various schemes over 200 random realizations.

To demonstrate the capability of estimating the transformer tap positions, the proposed methods are implemented on the system using the introduced equivalent models. After procuring the estimate states, the transformer tap position can be recovered by simply dividing the secondary side voltage by the primary side voltage for each transformer, while the tap position is pro-

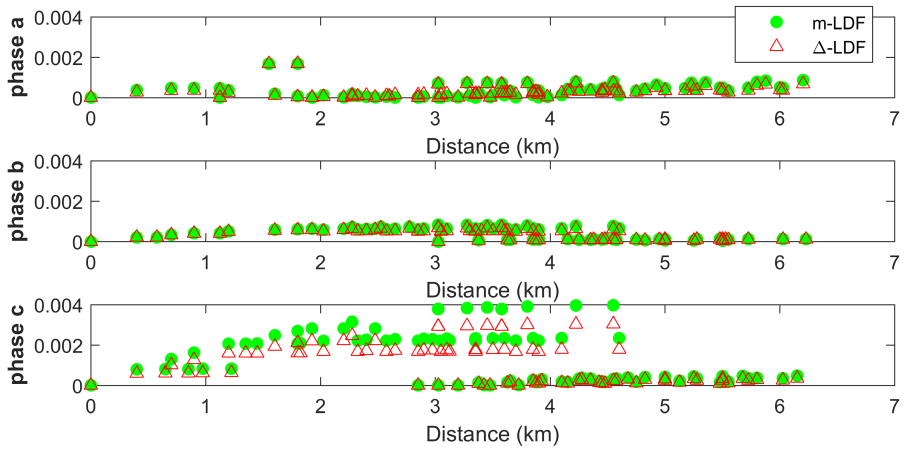

Figure 4.8: Voltage magnitude error results for the 123-bus system, by phase and distance

Table 4.4: The rMSE results of LDF-based SE schemes for the 123-bus system

rMSE	m-LDF	Δ-LDF	m-LDF w/ μPMU	Δ-LDF w/ μPMU
v	3.58×10^{-2}	3.27×10^{-2}	2.10×10^{-2}	2.08×10^{-2}
P	1.97×10^{0}	1.69×10^{0}	1.72×10^{0}	1.63×10^{0}
Q	2.55×10^{0}	2.16×10^{0}	2.23×10^{0}	2.08×10^{0}

vided by rounding the estimated ratio to the nearest discrete ratio. For one instance of the 123-bus results, Table 4.5 shows the actual and estimated transformer tap ratio and position by bus and phase. In this typical example, of the nine transformer taps in this scenario, only two were estimated to be different than their actual position. The effects of μPMU data on estimating the tap positions are also investigated. Figure 4.9 plots the percentage of the time that the estimation led to a certain number of incorrect tap positions, shown along the x-axis. It also compares the scenario of no μPMU data with that of having μPMU data at Bus 14, as before. This chart shows that if the estimation was incorrect, it was likely to be close (less than three positions off). Additional analysis shows that the estimation is more likely to be incorrect when the voltage references are far from each other, as the error accumulates over distance. This chart shows that introducing additional measurements, like those from a μPMU, can greatly increase the ability to accurately estimate the tap position, demonstrating

Table 4.5: Actual and estimated transformer tap ratio and position for one instance of the 123-bus results

Bus	Phase	Tap Ratio (Position)	Estimated Ratio (Position)	Difference
150	a	1.0375 (6)	1.0377 (6)	0.0002
	b	1.0375 (6)	1.0377 (6)	0.0002
	c	1.0375 (6)	1.0376 (6)	0.0001
9	a	1.0000 (0)	0.9971 (0)	0.0029
25	a	1.0125 (2)	1.0082 (1)	0.0043
	c	1.0000 (0)	0.9984 (0)	0.0015
160	a	1.0625 (10)	1.0611 (10)	0.0014
	b	1.0250 (4)	1.0251 (4)	0.0000
	c	1.0375 (6)	1.0340 (5)	0.0035

the value that even one μPMU can have in increasing the accuracy of the proposed distribution system SE.

The simulation results in this section show how the proposed models are effective for large-scale systems, provide flexibility with respect to measurement type, and ultimately effectively monitor the system state leveraging all available measurement information without inhibitive concerns such as solution convergence issues.

4.3 Chapter Summary

In this chapter, two DSSE methods were tested on various IEEE distribution feeder systems. Both exercised their specialized modeling and solution techniques to provide accurate estimates from a variety of input measurement sets in a manner that is both computationally efficient and immune to iteration-based ill-conditioning issues. In addition, the SDP-based method extension to bad data detection was validated as well as the LDF-based extension to estimating transformer tap position. These methods greatly benefit the task of monitoring the changing distribution system by enabling the integration of a diverse available measurement set without the consequences of numeric ill-conditioning and lack of convergence.

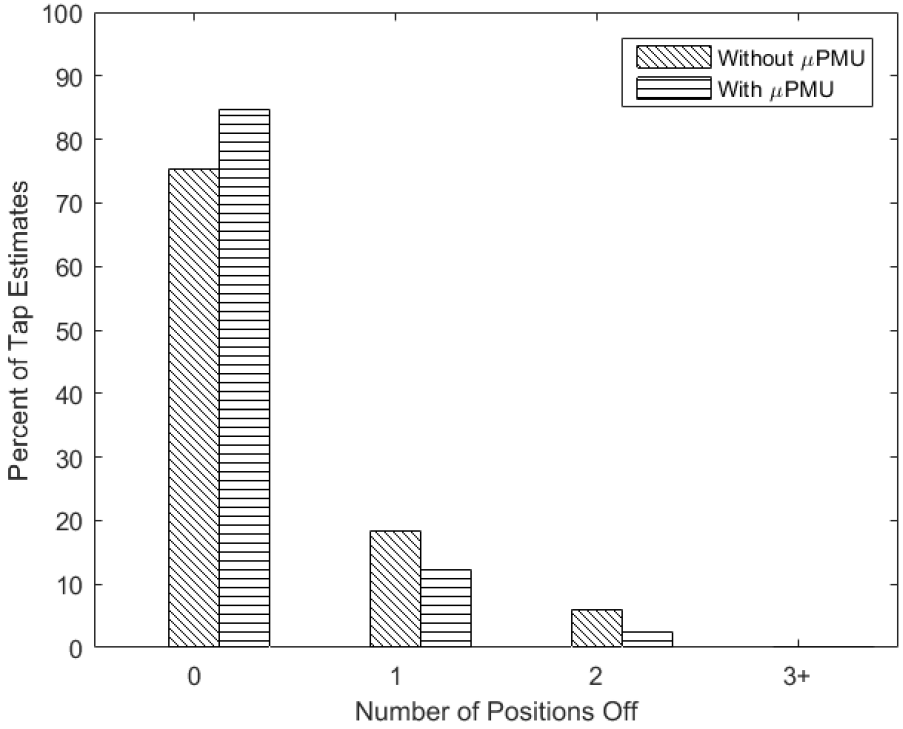

Figure 4.9: Percent of occurrences in erroneous tap estimation versus severity of error, with and without μPMU

CHAPTER 5

CONCLUSION

Motivated by the increasing need for effective monitoring tools for distribution networks, this thesis explores models and methods for distribution system power flow and state estimation. In an effort to take into consideration the unique characteristics and available measurements in distribution systems, two new multi-phase state estimation methods are proposed. Where many methods maintain the nonlinear power flow equations and solve the DSSE using iterative methods, the proposed techniques employ alternative power flow models to enable the use of semidefinite and quadratic programming solutions.

The methods are tested on the IEEE 13-bus and 123-bus systems under various conditions, including with bad data and varied measurement sets. The SDP-based state estimation method can seamlessly integrate virtual measurements using equality constraints and provide an estimate via convex solvers that is highly accurate on its own, or can be used as an initial guess for WLS. The LDF-based state estimation technique incorporates a constant approximate line difference term to improve upon the state estimate while maintaining the conveniently solvable form of the problem as a quadratic program with linear constraints. This method was also shown to successfully assimilate a variety of measurements, including metered, virtual, pseudo, and μPMU data.

Compared to the typical models and iterative methods, which are sensitive to factors that may cause ill-conditioning and solution divergence, the SDP-based and LDF-based DSSE methods successfully cast the SE problem as a semidefinite or quadratic program and thus provide a reliable, accurate, and robust state estimate in a computationally effective manner.

5.1 Future Work

Although these schemes have many advantages, additional improvements can be explored to further increase computational efficiency and robustness as the distribution network continues to evolve. For the SDP method, distributed algorithms will be explored to decrease the computation time, especially as the system size increases. Future work on the LDF methods will include scaling the problem to larger, more realistic systems and further analysis of how to best incorporate the widely-available current magnitude measurements.

REFERENCES

[1] G. Heydt, "The next generation of power distribution systems," *IEEE Transactions on Smart Grid*, vol. 1, no. 3, pp. 225–235, Dec 2010.

[2] A. Abur and A. Exposito, *Power System State Estimation: Theory and Implementation*. Mercel Dekker, 2004.

[3] A. Monticelli, "Electric power system state estimation," *Proceedings of the IEEE*, vol. 88, no. 2, pp. 262–282, Feb 2000.

[4] M. E. Baran, "Challenges in state estimation on distribution systems," *Power Engineering Society Summer Meeting*, vol. 1, pp. 429–433, July 2001.

[5] M. E. Baran and A. W. Kelley, "State estimation for real-time monitoring of distribution systems," *IEEE Transactions on Power Systems*, vol. 9, no. 3, pp. 1601–1609, Aug 1994.

[6] C. N. Lu, J. H. Teng, and W. H. E. Liu, "Distribution system state estimation," *IEEE Transactions on Power Systems*, vol. 10, no. 1, pp. 229–240, Feb 1995.

[7] W.-M. Lin and J.-H. Teng, "State estimation for distribution systems with zero-injection constraints," *IEEE Transactions on Power Systems*, vol. 11, no. 1, pp. 518–524, Feb 1996.

[8] M. E. Baran and A. W. Kelley, "A branch-current-based state estimation method for distribution systems," *IEEE Transactions on Power Systems*, vol. 10, no. 1, pp. 483–491, Feb 1995.

[9] H. Wang and N. N. Schulz, "A revised branch current-based distribution system state estimation algorithm and meter placement impact," *IEEE Transactions on Power Systems*, vol. 19, no. 1, pp. 207–213, Feb 2004.

[10] A. von Meier, D. Culler, A. McEachern, and R. Arghandeh, "Micro-synchrophasors for distribution systems," in *Innovative Smart Grid Technologies Conference (ISGT), 2014 IEEE PES*, Feb 2014, pp. 1–5.

[11] Y. Ju, W. Sheng, X. Song, J. Wang, and W. Wu, "Multi-phase distribution state estimation with only direct measurements," in *2015 5th International Conference on Electric Utility Deregulation and Restructuring and Power Technologies (DRPT)*, Nov 2015, pp. 2690–2694.

[12] X. Chen, K. J. Tseng, and G. Amaratunga, "State estimation for distribution systems using micro-synchrophasors," in *Power and Energy Engineering Conference (APPEEC), 2015 IEEE PES Asia-Pacific*, Nov 2015, pp. 1–5.

[13] D. A. Haughton and G. T. Heydt, "A linear state estimation formulation for smart distribution systems," *IEEE Transactions on Power Systems*, vol. 28, no. 2, pp. 1187–1195, May 2013.

[14] H. Ahmadi, J. R. Martí, and A. von Meier, "A linear power flow formulation for three-phase distribution systems," *IEEE Transactions on Power Systems*, vol. PP, no. 99, pp. 1–10, 2016.

[15] G. O. Alves, J. L. R. Pereira, P. A. N. Garcia, M. A. Souza, T. G. Moreira, P. S. C. Nascimento, and S. Carneiro, "Distribution system state estimation using phasor measurement units," in *2016 10th International Conference on Compatibility, Power Electronics and Power Engineering (CPE-POWERENG)*, June 2016, pp. 132–137.

[16] C. Muscas, M. Pau, P. A. Pegoraro, and S. Sulis, "Uncertainty of voltage profile in PMU-based distribution system state estimation," *IEEE Transactions on Instrumentation and Measurement*, vol. 65, no. 5, pp. 988–998, May 2016.

[17] J. Peppanen, M. J. Reno, M. Thakkar, S. Grijalva, and R. G. Harley, "Leveraging AMI data for distribution system model calibration and situational awareness," *IEEE Transactions on Smart Grid*, vol. 6, no. 4, pp. 2050–2059, July 2015.

[18] J. B. Leite and J. R. S. Mantovani, "Distribution system state estimation using the Hamiltonian cycle theory," *IEEE Transactions on Smart Grid*, vol. 7, no. 1, pp. 366–375, Jan 2016.

[19] D. Ablaković, I. Dzafić, R. A. Jabr, and B. C. Pal, "Experience in distribution state estimation preparation and operation in complex radial distribution networks," in *2014 IEEE PES General Meeting — Conference Exposition*, July 2014, pp. 1–5.

[20] I. Dzafić, R. A. Jabr, I. Huseinagic, and B. C. Pal, "Multi-phase state estimation featuring industrial-grade distribution network models," *IEEE Transactions on Smart Grid*, vol. PP, no. 99, pp. 1–1, 2016.

[21] E. Manitsas, R. Singh, B. C. Pal, and G. Strbac, "Distribution system state estimation using an artificial neural network approach for pseudo measurement modeling," *IEEE Transactions on Power Systems*, vol. 27, no. 4, pp. 1888–1896, Nov 2012.

[22] S. Nanchian, A. Majumdar, and B. C. Pal, "Three-phase state estimation using hybrid particle swarm optimization," *IEEE Transactions on Smart Grid*, vol. PP, no. 99, pp. 1–1, 2015.

[23] E. Manitsas, R. Singh, B. C. Pal, and G. Strbac, "Distribution system state estimation using an artificial neural network approach for pseudo measurement modeling," *IEEE Transactions on Power Systems*, vol. 27, no. 4, pp. 1888–1896, Nov 2012.

[24] T. C. Xygkis and G. N. Korres, "Optimal allocation of smart metering systems for enhanced distribution system state estimation," in *2016 Power Systems Computation Conference (PSCC)*, June 2016, pp. 1–7.

[25] M. G. Damavandi, V. Krishnamurthy, and J. R. Martí, "Robust meter placement for state estimation in active distribution systems," *IEEE Transactions on Smart Grid*, vol. 6, no. 4, pp. 1972–1982, July 2015.

[26] F. Meng, D. Haughton, B. Chowdhury, M. L. Crow, and G. T. Heydt, "Distributed generation and storage optimal control with state estimation," *IEEE Transactions on Smart Grid*, vol. 4, no. 4, pp. 2266–2273, Dec 2013.

[27] L. Schenato, G. Barchi, D. Macii, R. Arghandeh, K. Poolla, and A. V. Meier, "Bayesian linear state estimation using smart meters and PMUs measurements in distribution grids," in *Smart Grid Communications (SmartGridComm), 2014 IEEE International Conference on*, Nov 2014, pp. 572–577.

[28] M. G. Damavandi, V. Krishnamurthy, and J. R. Martí, "Robust meter placement for state estimation in active distribution systems," *IEEE Transactions on Smart Grid*, vol. 6, no. 4, pp. 1972–1982, July 2015.

[29] H. Zhu and G. Giannakis, "Power system nonlinear state estimation using distributed semidefinite programming," *IEEE Journal of Selected Topics in Signal Processing*, vol. 8, no. 6, pp. 1038–1050, Dec. 2014.

[30] L. Gan and S. H. Low, "Convex relaxations and linear approximation for optimal power flow in multiphase radial networks," in *Power Systems Computation Conference (PSCC), 2014*, Aug 2014, pp. 1–9.

[31] M. E. Baran and F. F. Wu, "Optimal capacitor placement on radial distribution systems," *IEEE Transactions on Power Delivery*, vol. 4, no. 1, pp. 725–734, Jan 1989.

[32] S. Bolognani and S. Zampieri, "On the existence and linear approximation of the power flow solution in power distribution networks," *IEEE Transactions on Power Systems*, vol. 31, no. 1, pp. 163–172, Jan 2016.

[33] S. V. Dhople, S. S. Guggilam, and Y. C. Chen, "Linear approximations to ac power flow in rectangular coordinates," in *2015 53rd Annual Allerton Conference on Communication, Control, and Computing (Allerton)*, Sept 2015, pp. 211–217.

[34] S. Bolognani and F. Dorfler, "Fast power system analysis via implicit linearization of the power flow manifold," in *2015 53rd Annual Allerton Conference on Communication, Control, and Computing (Allerton)*, Sept 2015, pp. 402–409.

[35] A. Garces, "A linear three-phase load flow for power distribution systems," *IEEE Transactions on Power Systems*, vol. 31, no. 1, pp. 827–828, Jan 2016.

[36] W. H. Kersting, *Distribution System Modeling and Analysis*. CRC Press, 2012.

[37] H. Zhu and H. J. Liu, "Fast local voltage control under limited reactive power: Optimality and stability analysis," *IEEE Transactions on Power Systems*, vol. PP, no. 99, pp. 1–10, 2015.

[38] R. D. Zimmerman, C. E. Murillo-Sanchez, and R. J. Thomas, "Matpower: Steady-state operations, planning, and analysis tools for power systems research and education," *IEEE Transactions on Power Systems*, vol. 26, no. 1, pp. 12–19, Feb 2011.

[39] "Distribution test feeders," http://ewh.ieee.org/soc/pes/dsacom/testfeeders.

[40] R. Dugan, "Open distribution system simulator (opendss)," http://smartgrid.epri.com/SimulationTool.aspx.

[41] V. Kekatos and G. B. Giannakis, "Joint power system state estimation and breaker status identification," in *North American Power Symposium (NAPS), 2012*, Sept 2012, pp. 1–6.

[42] P. Venkatesh, B. Manikandan, S. C. Raja, and A. Srinivasan, *Electrical Power Systems: Analysis, Security and Deregulation*. PHI Learning, 2012.

[43] R. A. Jabr, "Optimal power flow using an extended conic quadratic formulation," *IEEE Transactions on Power Systems*, vol. 23, no. 3, pp. 1000–1008, Aug 2008.

[44] B. A. Robbins, H. Zhu, and A. D. Domínguez-García, "Optimal tap setting of voltage regulation transformers in unbalanced distribution systems," *IEEE Transactions on Power Systems*, vol. 31, no. 1, pp. 256–267, Jan 2016.

[45] M. Grant and S. Boyd, "CVX: Matlab software for disciplined convex programming," http://cvxr.com/cvx, 2013.

[46] "The MOSEK optimization toolbox for Matlab," http://docs.mosek.com/7.1/toolbox, 2015.

[47] Y. Weng, Q. Li, R. Negi, and M. Ilić, "Distributed algorithm for SDP state estimation," in *Innovative Smart Grid Technologies (ISGT), 2013 IEEE PES*, Feb 2013, pp. 1–6.